

## PULSATION IN HOT MAIN SEQUENCE STARS: COMPARISON OF OBSERVATIONS WITH MODELS

L. A. BALONA

South African Astronomical Observatory, P.O. Box 9, Observatory 7935, Cape Town, South Africa  
*Version January 25, 2024*

### ABSTRACT

Comparison of *TESS* observations with models of pulsating hot main sequence stars reveals several problems. The frequencies in  $\delta$  Scuti stars at a given temperature do not match those predicted by models. A large fraction of  $\delta$  Scuti stars are hotter than the predicted hot edge of the instability strip. These Maia variables occupy a region in the H–R diagram between the  $\delta$  Scuti and  $\beta$  Cephei stars. Their high frequencies cannot be explained by rapid rotation. The  $\gamma$  Doradus stars are to be found together with  $\delta$  Scuti stars all along the main sequence where they merge with SPB stars. They are an example of the extraordinary frequency pattern variations seen in  $\delta$  Scuti stars, suggesting that the linear behaviour assumed in the models is incorrect. A well-defined upper envelope in frequency as a function of effective temperature is found in  $\delta$  Scuti and Maia variables. The frequencies of  $\beta$  Cephei stars are generally higher than predicted. The gap in the H–R diagram between  $\beta$  Cephei and hot SPB stars predicted by the models is not observed. Most  $\beta$  Cephei variables contain low frequencies typical of SPB stars. There are no discernible boundaries between the traditional classes of pulsating stars. A major revision of pulsation in upper main sequence stars is required.

*Subject headings:* stars: oscillations — stars: early-type — stars: variables: general — stars:  $\delta$  Scuti

### 1. INTRODUCTION

Prior to space observations, stellar pulsation among hot main sequence stars appeared to be well understood. The  $\delta$  Scuti (DSCT) variables are F5–A2 dwarfs or giants with frequencies 5–50 d<sup>−1</sup> in which pulsational driving is mostly attributed to the opacity  $\kappa$  mechanism operating in the He II partial ionization zone. For the cooler DSCT stars, coupling between convection and pulsation is important and affords an explanation for the  $\gamma$  Doradus (GDOR) variables (Dupret et al. 2005; Xiong et al. 2016). These are stars with pulsation frequencies less than 5 d<sup>−1</sup> lying on the cool edge of the DSCT instability strip.

The  $\beta$  Cephei (BCEP) variables, which are B4–O9 main sequence stars pulsating with frequencies in the range 3–20 d<sup>−1</sup>, are driven by the opacity mechanism operating in the partial ionization zone of iron-like metals. The same mechanism is responsible for the SPB stars which have frequencies less than 3 d<sup>−1</sup>. In these less massive stars, the iron opacity bump is located in a deeper layer. Together with the lower luminosity, this leads to an increase in the thermal timescale and lower pulsation frequencies. These SPB stars partially overlap the BCEP variables and extend to spectral type B8. Between the cool edge of the SPB variables and the hot edge of the DSCT stars, models do not predict pulsation.

Photometric time-series observations from space missions such as *CoRoT*, *Kepler* and *TESS* have increasingly challenged the above perceptions. From *CoRoT* observations, Degroote et al. (2009) reported low-amplitude late B-type pulsators lying between the SPB and DSCT

instability strips with frequencies similar to those in DSCT stars. Such “Maia” variables, as they have historically been called, had been suspected from ground-based photometry (McNamara 1985; Lehmann et al. 1995; Percy and Wilson 2000; Kallinger et al. 2004). The existence of MAIA variables is now well established, not only from *Kepler* and *TESS* missions (Balona and Ozuyar 2020a; Balona 2023), but also from *Gaia* photometry (Gaia Collaboration et al. 2023).

The general view is that MAIA variables do not constitute a new group of pulsating stars. The high frequencies are presumed to be gravito-inertial modes shifted to high frequencies in rapidly rotating SPB stars (Townsend 2005; Salmon et al. 2014). However, an analysis of their projected rotational velocities shows that MAIA stars have the same rotational velocity distribution as main sequence stars. In addition, over 10% of MAIA variables have frequencies exceeding 60 d<sup>−1</sup>, which certainly cannot be a result of rotation. The MAIA variables appear to be an extension of the DSCT variables to early B stars (Balona 2023).

Gravito-inertial modes have been detected in several stars (Pápics et al. 2012; Van Reeth et al. 2018; Mombarg et al. 2019; Ouazzani et al. 2020). These seem to be present, together with acoustic gravity modes, in GDOR stars. They arise in rotating stars where the Coriolis force acts as a restoring force. Rossby waves are seen as broad features in the periodograms of some DSCT variables (Saio et al. 2018). Mirouh (2022) has presented an excellent review of the various types of oscillations that may be present in rotating stars.

Models do not predict low frequencies for main sequence stars with effective temperatures in the range

$7500 < T_{\text{eff}} < 11\,000$  K. Yet there are a substantial number of GDOR stars hotter than 7500 K (Balona et al. 2016). The GDOR and SPB stars form a continuous group of low-frequency variables. Whether or not pulsation in these hot GDOR stars may be attributed to inertial modes is an open question. Low frequencies are also present in most DSCT stars hotter than about 7500 K (Grigahcène et al. 2010). These used to be known as DSCT+GDOR “hybrids”, but since most DSCT stars are hybrids, the term is no longer useful.

The rapidly-oscillating Ap (roAp) stars are Ap/Fp main sequence stars that pulsate in a limited high-frequency range above  $60\text{ d}^{-1}$  (Kurtz 1982). Until recently, such high frequencies were assumed to be confined to chemically peculiar stars, but data from the *TESS* mission has shown that similar frequencies occur in many chemically normal stars (Balona 2022a). It appears that roAp stars should not be regarded as a separate class but as ordinary members of the DSCT class.

The mass loss in Be stars is frequently attributed to pulsation. However, the quasi-periodic light variations are not coherent, as expected from a pulsating star. There is a characteristic pattern in the light curves and periodograms of Be stars which can be understood as a result of co-rotating circumstellar clouds (Balona and Ozuyar 2020b, 2021). Be stars are not considered in this paper.

It turns out that there are no clear boundaries between any of the several types of hot pulsating stars GDOR, DSCT, MAIA, SPB and BCEP (Balona and Ozuyar 2020a). This complicates the definition of the variability classes because arbitrary boundaries in effective temperature and frequency need to be introduced to uniquely define each variability class.

A very strange aspect is the huge variety of frequency patterns to be found in DSCT stars with similar effective temperatures, luminosities, and rotation rates (Balona 2024). Stars with similar parameters should pulsate with similar frequencies and amplitudes, as models predict. This appears not to be the case. Each DSCT star has a unique frequency pattern.

Non-adiabatic pulsation models assume that pulsation is a linear phenomenon at very low amplitudes. A mode that is unstable at a given frequency is assumed to grow to a limiting amplitude while maintaining nearly the same pulsation frequency. It seems that this fundamental assumption is not correct for DSCT stars (and perhaps for other classes as well). As a result, the frequency that is observed is probably a result of a non-linear interaction and bears no resemblance to the frequency predicted by the models (Mourabit and Weinberg 2023).

It seems that current perceptions of stellar pulsation in hot main sequence stars, which were adequate to explain ground-based observations, are no longer sufficient. This paper aims to compare the predicted location of pulsation instability and the frequencies with *TESS* observations of hot main sequence stars. In this way, one might obtain clues as to how the models could be modified to better agree with observations. This work is based on a catalogue of the variability classes of over 125 000 *Kepler* and *TESS* stars on the upper main sequence compiled by Balona (2022b) which is freely available.

## 2. THE DATA AND VARIABILITY CLASSIFICATION

The light curves obtained from the *Kepler* and *TESS* missions were used to construct periodograms. By inspecting the light curves and periodograms and knowing the approximate location of a star in the H–R diagram from its effective temperature or spectral type, a variability class can be assigned. The results described here are from *TESS* sectors 1–68.

DSCT stars are defined to be main sequence F or A stars ( $6000 < T_{\text{eff}} < 10\,000$  K) which pulsate with high frequencies. In this respect, “high frequency” is taken to mean any frequency higher than  $5\text{ d}^{-1}$ . Lower frequencies may, or may not, be present. If only frequencies less than  $5\text{ d}^{-1}$  are present, the star is classified as GDOR.

Stars with frequencies less than  $5\text{ d}^{-1}$  and in the temperature range  $10\,000 < T_{\text{eff}} < 18\,000$  K are classified as SPB. SPB variables also include stars with  $T_{\text{eff}} > 18\,000$  K, but in this temperature range the maximum frequency is restricted to less than  $3\text{ d}^{-1}$ . This is necessary because BCEP stars may have frequencies as low as  $3\text{ d}^{-1}$ .

Stars with  $T_{\text{eff}} > 18\,000$  K and at least one frequency peak higher than  $3\text{ d}^{-1}$  are defined as BCEP. BCEP stars with low frequencies are classified as BCEP+SPB hybrids, but this may not be necessary as most BCEP stars are “hybrids” anyway.

Main sequence stars with  $10\,000 < T_{\text{eff}} < 18\,000$  K and frequencies higher than  $5\text{ d}^{-1}$  are defined as MAIA variables. It is not possible to distinguish between MAIA and DSCT stars without introducing a temperature boundary. The value of  $T_{\text{eff}} = 10\,000$  K is convenient, being the boundary between the A- and B-type stars.

In addition to *TESS* photometry, linear non-adiabatic models were calculated so that the predicted frequencies and location in the H–R diagram could be compared with the observations. Evolutionary stellar models were computed using the Warsaw - New Jersey evolution code (Paczynski 1970), assuming an initial hydrogen fraction,  $X_0 = 0.70$  and metal abundance,  $Z = 0.020$  and using the chemical element mixture of Asplund et al. (2009) and OPAL opacities (Rogers and Iglesias 1992). Overshooting from the convective core was not included. A mixing length parameter  $\alpha_{\text{MLT}} = 1.0$  was adopted for the convective scale height. All models are non-rotating. The non-adiabatic code developed by Dziembowski (1977) was used to obtain the pulsation frequencies and growth rates. These models will be called the “Dziembowski” models.

## 3. LOCATION IN THE H–R DIAGRAM

Comparison of the location and extent of the observed and predicted instability strips is an important test of the models. The location in the H–R diagram of BCEP, SPB, DSCT, and GDOR stars is shown in the left panels of Fig. 1. Also shown are the theoretical instability strips of BCEP and SPB stars from Miglio et al. (2007b) and the hot and cool edges of the DSCT and GDOR instability strips from Dupret et al. (2005) and Xiong et al. (2016). The panels on the right show the location in the H–R diagram of the Dziembowski models with unstable modes as well as the theoretical instability strips.

The most obvious discrepancy is existence of the MAIA class of variables which is not predicted by the models. The large number of DSCT stars hotter than the theoretical hot edge of the instability strip also presents a

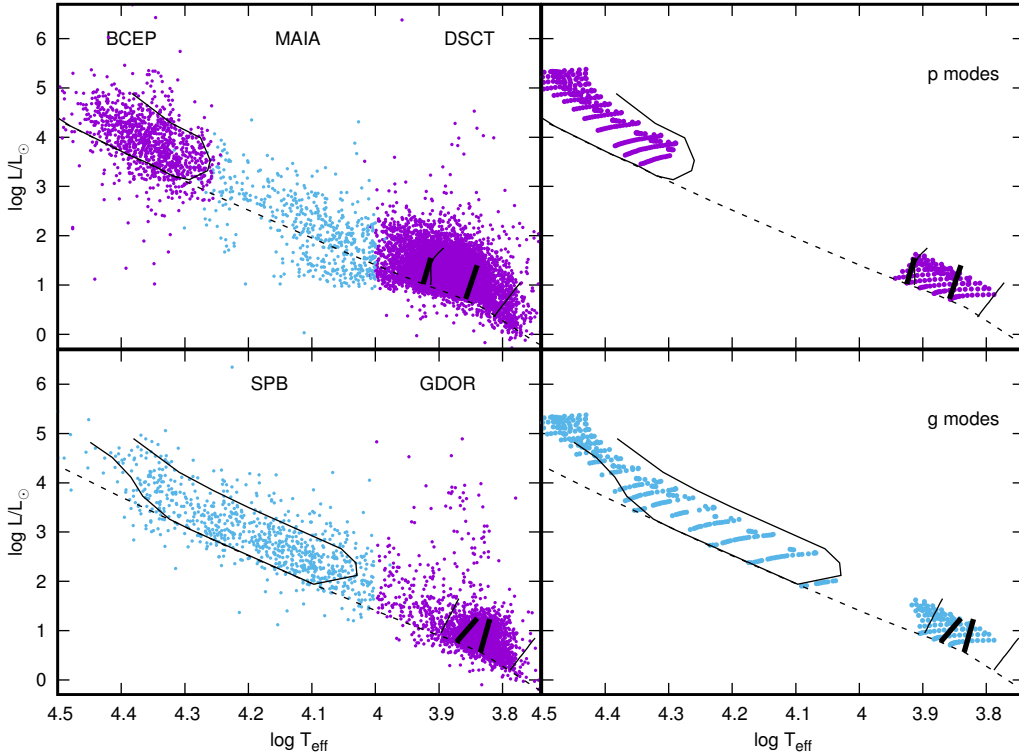


FIG. 1.— The location of various classes of pulsating stars in the H-R diagram (left panels) and location of Dziembowski models showing unstable p and g modes (right panels). The dashed line is the zero-age main sequence. Also shown are the instability regions in BCEP and SPB stars for solar abundance models by Miglio et al. (2007a) and the hot and cool edges of the DSCT and GDOR stars from Dupret et al. (2005) (thick lines) and Xiong et al. (2016) (thin lines).

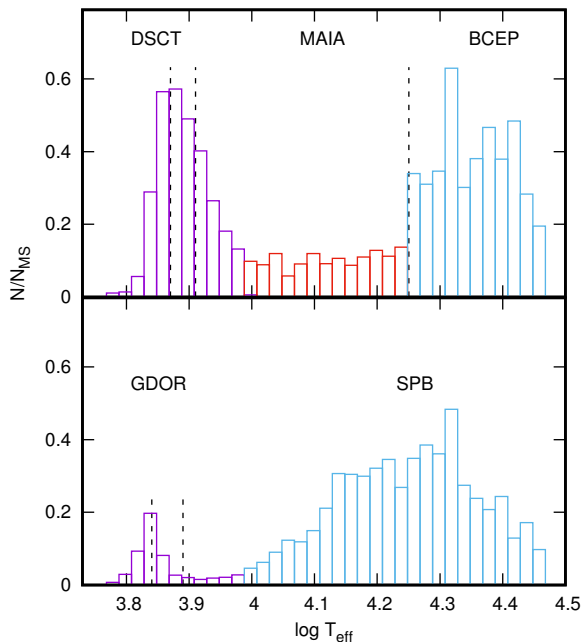


FIG. 2.— The ratio  $N/N_{\text{MS}}$  as a function of effective temperature.  $N$  is the number of stars of the particular variability class and  $N_{\text{MS}}$  is the number of main sequence stars within the temperature bin size. The vertical dashed lines indicate the minimum and maximum temperature of the hot edge of DSCT and GDOR stars predicted by various models. The cool edge of the BCEP instability region from Miglio et al. (2007b) is shown.

serious problem. The continuous band of low-frequency main sequence stars between the cool end of the SPB instability strip and the hot end of the GDOR instability strip should also be noted.

The number density of stars decreases rapidly with effective temperature. Whereas F0 stars are very common, B0 stars are very rare. Fig. 1 therefore gives a somewhat biased view of the relative number of stars of different variability classes. The fraction of stars of a given variability class relative to the number of main sequence stars at a particular temperature is shown in Fig. 2.

Over 500 MAIA variables have been classified from *TESS* photometry. The figure shows that MAIA variables comprise more than 10% of mid- to late-B stars and are relatively more numerous than GDOR stars. The figure also shows that the large majority of main sequence stars do not seem to pulsate at all, or at least do not pulsate with amplitudes that can be detected by *TESS*. This, too, is not understood.

Fig. 2 shows how poorly the theoretical hot edge of DSCT stars agrees with observations. It also shows how the relative numbers of DSCT stars match smoothly with those of MAIA variables. The MAIA stars seem to be just an extension of the DSCT variables. The figure also illustrates the continuity between GDOR and SPB stars.

#### 4. PULSATION FREQUENCIES

In the previous section, it was shown that pulsation models fail to correctly predict the hot edge of the DSCT instability region, the MAIA stars or the large number of low-frequency pulsators between the SPB and GDOR

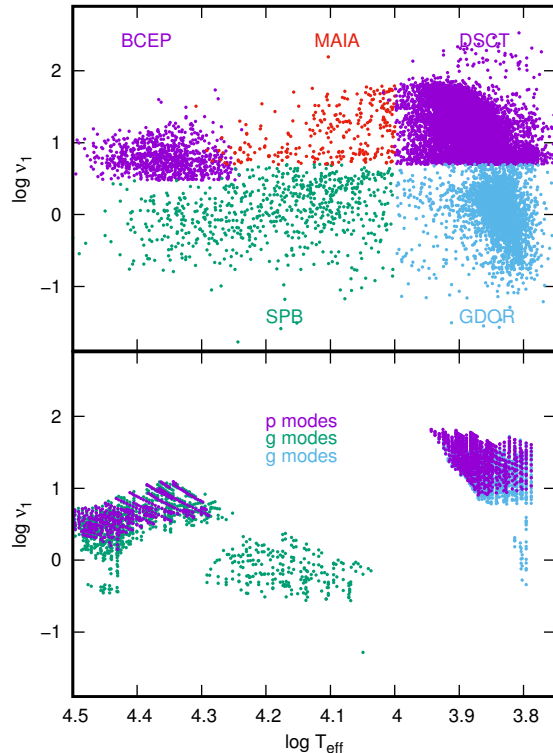


FIG. 3.— The top panel shows the frequency of largest amplitude of various types of *TESS* pulsating stars as a function of effective temperature. The bottom panel shows the frequencies of unstable modes with  $l \leq 2$  in non-rotating Dziembowski models.

instability strips. In this section, the frequencies of unstable modes from models are compared to the observed frequencies.

In the top panel of Fig. 3, the frequency of largest amplitude,  $\nu_1$ , is shown as a function of effective temperature. This may be compared with the frequencies of unstable modes with  $l \leq 2$  in non-rotating Dziembowski models (bottom panel). There are important discrepancies between observations and the models. The difference between the observed and predicted frequencies in GDOR stars is understandable because the adoption of frozen-in convection in the models is not very satisfactory. This should not affect models of the hotter stars where convection may perhaps be less important. The models do not show the low frequencies which are present in DSCT stars hotter than about 7500 K. The models also fail to reproduce the low frequencies in BCEP stars. The distinctive frequency gap between the BCEP and the SPB stars in the models does not exist.

The top panel of Fig. 3 shows a surprisingly well-defined upper frequency envelope in DSCT stars. The frequency of maximum amplitude,  $\nu_1$ , increases with temperature, reaching a maximum at about  $\log T_{\text{eff}} \approx 3.93$  before decreasing. The decrease in  $\nu_1$  continues in the MAIA stars. This is shown in more detail for the DSCT stars in the top panel of Fig. 4. The bottom panel shows unstable p and g modes from the Dziembowski models. The schematic envelope in this figure is reproduced in the top panel (blue line). Also shown in the top panel is the schematic envelope of p-mode frequencies with the highest growth rate from Fig. 9 of Xiong et al.

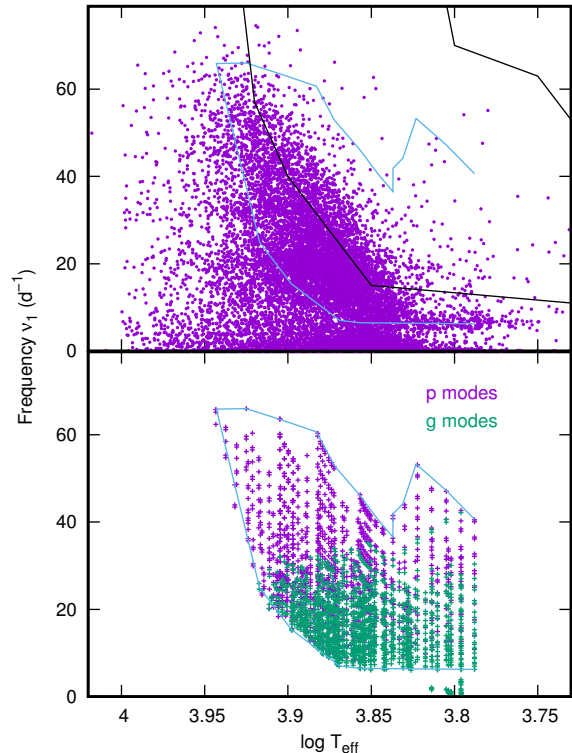


FIG. 4.— The top panel shows the frequency of maximum amplitude as a function of effective temperature for DSCT stars. The black outline is the envelope of the highest amplitude growth rate of low-degree p modes shown in Fig. 9 of Xiong et al. (2016). The blue outline is the envelope of unstable modes from Dziembowski models. The frequencies of unstable modes in the Dziembowski models is shown in the bottom panel.

(2016) (black line).

The frequencies of DSCT stars derived by Xiong et al. (2016) are in very poor agreement with observations. The frequencies from the Dziembowski models are in somewhat better agreement, but far from satisfactory. For  $\log T_{\text{eff}} > 3.87$ , low frequencies are stable in the Dziembowski models, whereas observations show that DSCT stars with low frequencies are the rule rather than the exception, as already noted above.

It does not matter whether the frequency of the largest amplitude,  $\nu_1$ , or second-largest amplitude,  $\nu_2$ , or the frequency with the  $n$ -th largest amplitude,  $\nu_n$ , is used. The upper envelope of frequency as a function of effective temperature is always surprisingly sharp. The frequency of the envelope at constant temperature increases slowly with  $n$ .

If, instead, the maximum frequency,  $\nu_{\text{max}}$ , is plotted as a function of effective temperature, the result is similar to Fig. 4, except that the envelope is shifted towards higher frequencies by about 20%. This is still considerably lower than the estimated critical frequency, which is the frequency beyond which the pulsational acoustic waves are no longer reflected in the atmosphere.

##### 5. IS THE GDOR CLASS NECESSARY?

The frequency threshold of  $\nu_t = 5 \text{ d}^{-1}$ , used to distinguish between DSCT and GDOR stars has no basis in theory. It was adopted because frequencies lower than  $5 \text{ d}^{-1}$  were never seen in ground-based photometry of

DSCT stars. This is not surprising because variations in atmospheric extinction and low pulsation amplitudes make the detection of low frequencies very difficult from the ground.

The detection of multiple low-frequency peaks in GDOR stars was unexpected and not predicted from the pulsation models available at that time. For this reason, it was presumed to be a new class of pulsating variable (Balona et al. 1994). Many more GDOR stars were subsequently discovered (Henry et al. 2007). However, there was no similar attempt to detect low frequencies in the DSCT stars known at the time.

The first example of “hybrid” DSCT+GDOR pulsation was discovered by Handler et al. (2002). Until the advent of space photometry, only 6 hybrids and 66 GDOR stars were known. Surprisingly, the first *Kepler* release revealed that most DSCT stars were hybrids (Grigahcène et al. 2010). Indeed, among the *TESS* DSCT stars, about 75% are hybrids.

In retrospect, it seems that if sufficient photometric precision were available, ground-based observations would have detected low frequencies in most DSCT stars at an early stage. In that case, the definition of DSCT stars would not have excluded low frequencies. What we now call GDOR stars would not have been a surprise and most likely regarded simply as DSCT stars with low frequencies.

Guzik et al. (2000) proposed the convective blocking mechanism to explain the low frequencies in GDOR stars. Later, Dupret et al. (2005) and Xiong et al. (2016) showed that the GDOR stars as well as low frequencies in the cooler DSCT stars could be modeled using a time-dependent convection theory. Xiong et al. (2016) concluded that there is no essential difference between DSCT and GDOR stars. They can be considered as just two subgroups of one broader variability class.

Since there seems no need to differentiate between DSCT and GDOR stars in the models, it seems appropriate to re-evaluate the relevance of a separate GDOR class. Fig. 5 shows the DSCT and GDOR stars in the H–R diagram. For convenience, the boundary of the DSCT and GDOR stars is approximated by a trapezoid (green) and triangle (orange) respectively. Most GDOR stars are located inside the triangular region on the cool side of the DSCT stars, more or less within the region of low-frequency g-mode instability predicted by Xiong et al. (2016). The models by Dupret et al. (2005) predict a much smaller region.

There are 3995 DSCT stars and 3237 GDOR stars inside the triangular GDOR region. In other words, there are as many DSCT stars as GDOR stars. The presence of GDOR and DSCT stars occupying the same region of the H–R diagram is impossible to duplicate in pulsation models. Furthermore, there is a large number of GDOR stars outside the main triangular region, extending well beyond the hot edge of DSCT stars. This, too, cannot be explained by current models. Furthermore, there are 35 792 *TESS* main sequence stars within the triangular GDOR region that are not observed to pulsate at all. The presence of stars with high frequencies, stars with low frequencies, and ostensibly non-pulsating stars in the same region of the H–R diagram is not understood. Models predict that all stars should pulsate.

Suppose that a threshold frequency,  $\nu_t$ , is used to dis-

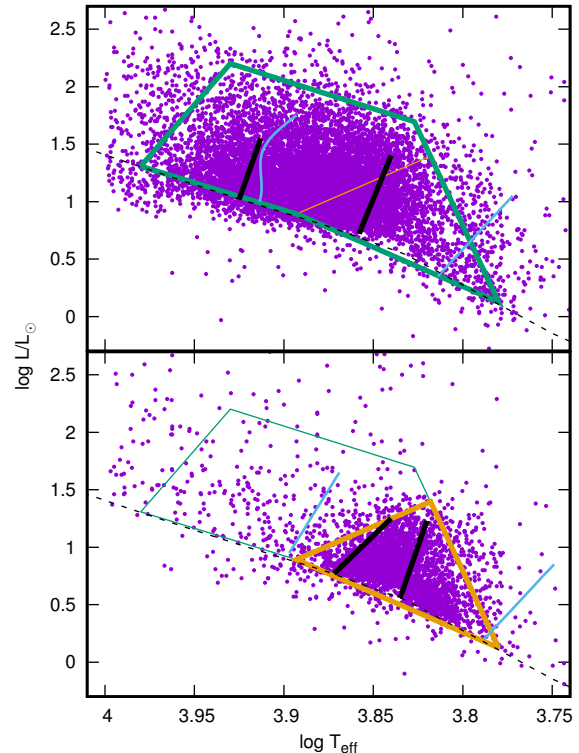


FIG. 5.— The top panel shows the location of 12772 *TESS* DSCT stars in the H–R diagram enclosed by a schematic trapezium (green). The hot and cool edges from Dupret et al. (2005) (thick black lines) and Xiong et al. (2016) (thin blue lines). The bottom panel shows 4065 *TESS* GDOR stars enclosed by schematic triangle (orange) and corresponding hot and cool edges. The diagonal dashed line is the zero-age main sequence.

criminate between GDOR and DSCT stars. Let  $n$  be the number of significant frequency peaks below  $\nu_t$ . If there is any significance to  $\nu_t$ , then one might hope to detect a difference in the distribution of  $n$  as a function of  $\nu_t$ . When this procedure is carried out with  $\nu_t = 4, 6, 8$  and  $10 \text{ d}^{-1}$ , it is found that the distributions of  $n$  are very similar. This suggests that there is no reason to regard stars with low frequencies as different from normal DSCT stars.

Recently, it has been established that there is an extraordinary range in frequency patterns among stars classified as DSCT (Balona 2024). This is at variance with the linear assumption which underlies all current pulsation models. The fact that DSCT and GDOR stars can be found in the same region of the H–R diagram is probably a result of non-linear mode excitation.

## 6. CONNECTION BETWEEN DSCT AND MAIA

Balona (2023) has shown that there is no difference in mean rotation rates of MAIA stars and normal main sequence stars and that the amplitude distribution of MAIA variables is the same as in DSCT stars, but different from BCEP stars. One may as well regard MAIA stars as an extension of DSCT variables to hotter temperatures. However, this conclusion awaits a theory that explains pulsation in DSCT stars hotter than the currently predicted limit as well as unstable high-frequency modes in late- to early-B stars.

The left panels of Fig. 6 show  $\nu_1$ , the frequency of max-

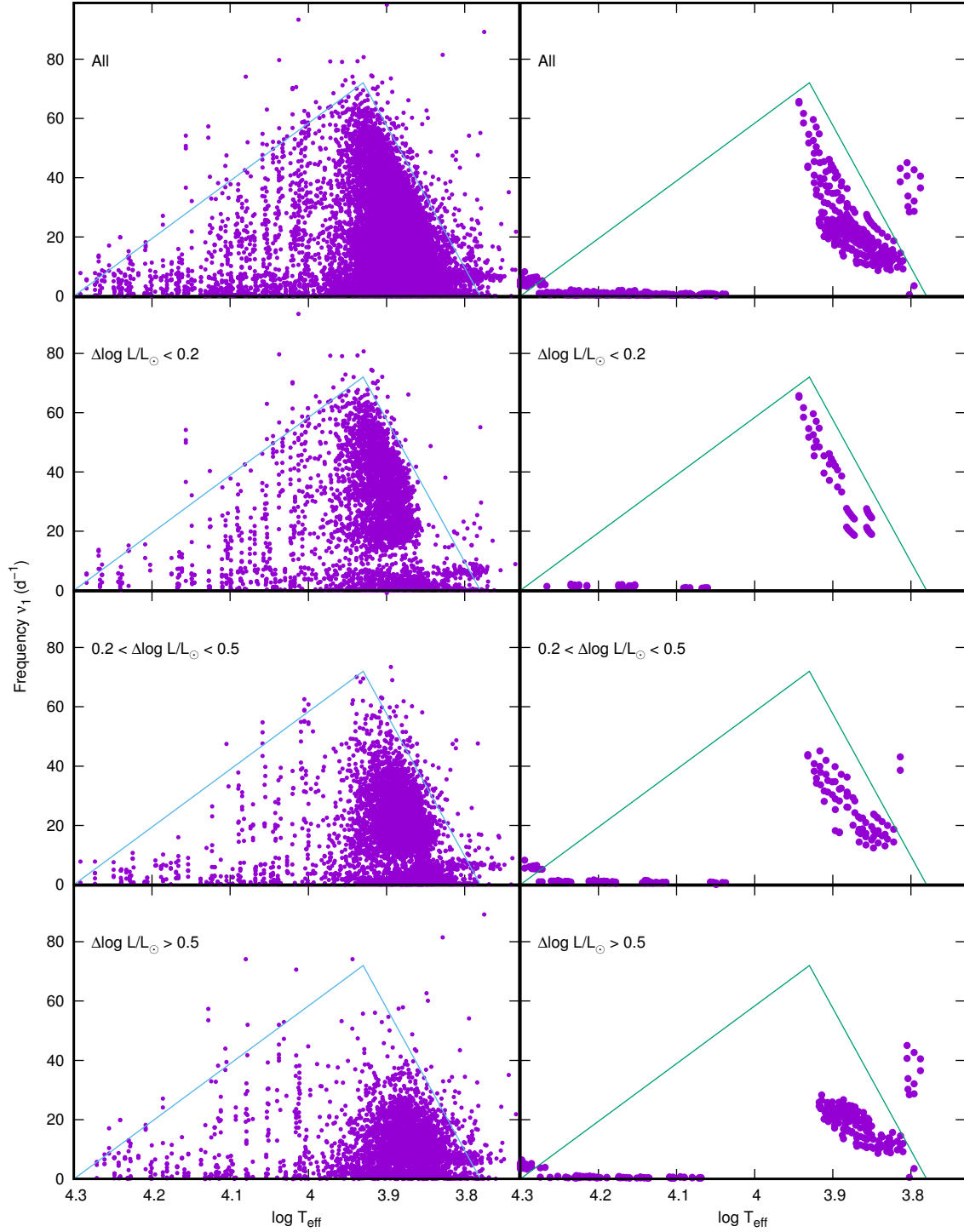


FIG. 6.— The frequency of maximum amplitude as a function of effective temperature. The top left panel shows all DSCT and MAIA stars enclosed by a triangular envelope. The other panels on the left show stars selected according to  $\Delta L/L_{\odot}$ , the luminosity above the zero-age main sequence. The panels on the right are the corresponding frequencies from the Dziembowski models.



imum amplitude, as a function of effective temperature for DSCT and MAIA stars. For MAIA stars, the plot shows  $\nu_1$ – $\nu_5$ , the frequencies of the five highest amplitude peaks. This is to balance the large difference in number density between the two classes.

The top left panel of Fig. 6 shows that there is a roughly linear increase in  $\nu_1$  from the coolest DSCT stars, reaching a maximum of about  $72 \text{ d}^{-1}$  at  $\log T_{\text{eff}} \approx 3.93$ . Thereafter the frequency decreases with temperature, reaching a minimum at the hot end of the MAIA variables, as shown by the blue lines in the figure. The systematic decrease in  $\nu_1$  initiated in the hot DSCT stars and continued by the MAIA variables seem to be another link between DSCT and MAIA stars.

The top right panel of Fig. 6 shows the frequencies  $\nu_1$ ,  $\nu_2$ , of the first two unstable modes of highest growth rate and visibility as a function of temperature from the Dziembowski models. Not surprisingly, nearly all the modes in this plot are radial with radial order increasing with frequency from 1 to 8. The increase in frequency with increasing temperature is also visible in the models.

Fig. 6 also shows the  $\nu_1$ – $\log T_{\text{eff}}$  diagram for stars in different luminosity ranges,  $\Delta L/L_{\odot}$ , above the zero-age main sequence (ZAMS). As  $\Delta L/L_{\odot}$  increases, the frequency of maximum amplitude decreases from  $72 \text{ d}^{-1}$  near the ZAMS to about  $40 \text{ d}^{-1}$  for the most evolved stars. The corresponding effective temperature at maximum frequency decreases from 8500 K for stars close to the ZAMS, to about 7500 K for more evolved stars. A similar behaviour seems to be present in the Dziembowski models (right panels in the figure).

The relationship between effective temperature and frequency in DSCT stars has been investigated by many authors. Barceló Forteza et al. (2018, 2020) found a linear relationship between an amplitude-weighted frequency and  $T_{\text{eff}}$  in DSCT stars. Bowman and Kurtz (2018) found a similar relationship for the frequency of maximum amplitude. However, as can be seen from the above figures, there is no unique relationship between  $\nu_1$  and  $\log T_{\text{eff}}$ .

## 7. THE SPB AND BCEP STARS

Unless colours in the  $U$  band are available, it is not possible to distinguish between the effect of temperature and interstellar reddening in B stars. Since modern CCDs are not sensitive in the  $U$  band, one has to rely mostly on spectroscopic estimates of effective temperature or estimates from Strömgren or Geneva photometry. The proportion of B stars with reliable effective temperatures is therefore considerably smaller than in A or F stars. The spectral type and luminosity class often provide the only reliable estimate of  $T_{\text{eff}}$  for B stars. Spectroscopy of B stars, such as those by Bursens et al. (2020) and Shi et al. (2023) are very important.

The defined lower bound in effective temperature for SPB stars,  $T_{\text{eff}} = 10\,000 \text{ K}$ , is less than the cool edge derived from models of non-rotating SPB stars by about 1000 K. It has been shown that SPB stars cooler than the theoretical cool edge do not rotate at a significantly higher rate than normal main sequence stars (Balona 2023). Rapid rotation cannot therefore be used to explain the presence of SPB stars beyond the cool edge. Stars with frequencies typical of SPB or GDOR stars occur all along the main sequence. Models fail to reproduce

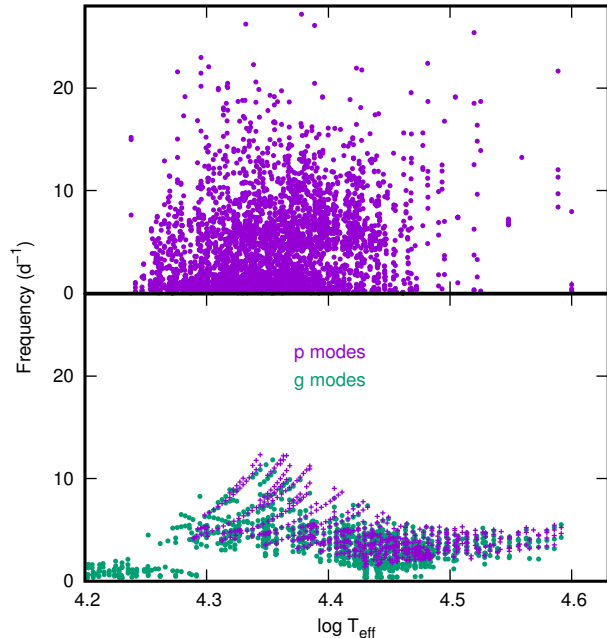


FIG. 7.— All observed frequencies in BCEP, BCEP+SPB or pure SPB stars in the BCEP temperature range are shown in the top panel. The bottom panel shows unstable modes for  $l \leq 2$  from Dziembowski models.

this continuous sequence of low-frequency pulsators.

In the catalog of Stankov and Handler (2005), there are 93 confirmed BCEP variables. An additional 103 BCEP stars are found in the photometric survey by Pigulski and Pojmański (2008). To these can be added the 86 new BCEP variables discovered by Labadie-Bartz et al. (2020), for a total of 282 known BCEP stars. In Balona (2022b), 800 new BCEP stars have been detected, bringing the total to 1082 BCEP stars identified from *TESS* photometry. Of these, 621 are classified as BCEP+SPB hybrids.

Hybrid BCEP+SPB pulsators were first discovered from ground-based photometry (Jerzykiewicz et al. 2005; Handler et al. 2006; Chapellier et al. 2006) and many more from space photometry (Degroote et al. 2010; Balona et al. 2011). From *TESS* data, 57% of BCEP stars are classified as BCEP+SPB hybrids.

The problem with BCEP+SPB hybrids is not merely a problem of classification. According to models, BCEP stars should not pulsate with frequencies lower than about  $3 \text{ d}^{-1}$ . This is because g modes have high amplitudes in the core and are heavily damped. The structure of the eigenfunction does play a role and, for some modes, driving can exceed damping in the inner layers.

To model the low frequencies requires an increase in opacity by about a factor of four (Pamyatnykh et al. 2004). The discrepancy between the models and observations may also be reduced, to some extent, by a choice of OP opacities rather than OPAL opacities (Dziembowski and Pamyatnykh 2008; Miglio et al. 2007b). Enhanced iron opacity to address this problem is discussed by Moravveji (2016).

The problem can be seen in the bottom panel of Fig. 3 or the bottom panel of Fig. 7. There is a distinct frequency gap between non-rotating models of SPB stars and BCEP stars, whereas no such gap appears in the ob-

servations. There are no unstable frequencies less than  $3 \text{ d}^{-1}$  for BCEP stars cooler than  $\log T_{\text{eff}} \approx 4.40$ .

Rapid rotation tends to lower pulsation frequencies and may also play a part in explaining the BCEP+SPB hybrids. In that case, pure BCEP stars should rotate more slowly than BCEP+SPB hybrids. From 123 pure BCEP stars  $\langle v \sin i \rangle = 113 \pm 8 \text{ km s}^{-1}$  and from 354 BCEP+SPB stars  $\langle v \sin i \rangle = 158 \pm 6 \text{ km s}^{-1}$ . The difference in rotation rate is not very large and more evidence is required.

The top panel of Fig. 7 shows the complete set of frequencies observed in BCEP, BCEP+SPB, and pure SPB stars in the BCEP temperature range as a function of effective temperature. The upper envelope is quite well defined, reaching a maximum frequency of about  $18 \text{ d}^{-1}$  at  $T_{\text{eff}} \approx 22\,000 \text{ K}$ . However, frequencies in the non-rotating models (bottom panel) do not exceed  $13 \text{ d}^{-1}$ . In spite of this discrepancy, BCEP stars show the best agreement with pulsation models.

#### 8. SOME UNUSUAL BCEP STARS

TIC 115642252 (NGC 1960 109). The field of this B2I 10.7 mag star is rather crowded and likely contaminated by TIC 115642245 (9-th magnitude). Nevertheless, this will not explain three high-frequency peaks (60.996, 57.189 and  $53.875 \text{ d}^{-1}$ ) present in TIC 115642252 but absent in TIC 115642245. Anders et al. (2022) list a photometric effective temperature of  $11\,174 \text{ K}$ , which conflicts with the spectral type and is possibly unreliable.

TIC 119462263 (HD 133518) is a He-strong star (B2IVp) (Zboril and North 2000) with high magnetic field strength (Alecian et al. 2014). The pulsation frequencies are  $57.391$  and  $54.169 \text{ d}^{-1}$  with a possible third peak at  $60.727 \text{ d}^{-1}$ . These frequencies are much higher than generally seen in BCEP stars. Although the field is quite crowded, the star is very bright ( $V = 6.4$  mag) and other stars within a 2 arcmin field of view are fainter than 10-th magnitude.

TIC 304425262 (HD 103079) is a very bright ( $V = 4.9$ ) B4IV star. Apart from frequencies that qualify it as BCEP+SPB, there is also an interesting set of 8 peaks between  $55$  and  $62 \text{ d}^{-1}$ . The possibility that these are artifacts owing to the star's brightness cannot be ruled out.

#### 9. CONCLUSIONS

In this paper, the observed regions of instability in the H–R diagram for various classes of pulsating stars and their frequencies are compared with predictions from pulsation models. It is concluded that, except possibly for BCEP stars, the models are in poor agreement with observations.

The origin of the high frequencies in MAIA variables has frequently been dismissed as due to rotation, even though Balona and Ozuyar (2020a) have shown that the projected rotational velocities of MAIA stars are no different from main sequence stars in the same effective temperature range. More recently, Balona (2023) has shown that the  $v \sin i$  distribution of 145 MAIA stars agrees with the  $v \sin i$  distribution of 6538 main sequence stars in the same temperature range. In any case, rapid rotation will not explain frequencies over  $60 \text{ d}^{-1}$  which occur in about 10 % of MAIA stars. The amplitude distribution of MAIA variables is also the same as DSCT stars (Balona 2023), showing that MAIA stars are not DSCT

variables in B-star binaries. The driving mechanism for these hot DSCT stars is unknown and should be considered a major unsolved problem.

Another major problem is that DSCT stars do not behave as predicted at a fundamental level. It is taken for granted that stars with the same effective temperature, luminosity, and rotation rate should have the same frequencies. Moreover, slight changes in stellar parameters should lead to only slight changes in the pulsation frequency spectra. Observations show very different behaviour. The frequency patterns in DSCT stars with similar parameters exhibit an extreme variety (Balona 2024). This suggests that mode selection is a highly non-linear process mostly determined by local conditions.

There are serious discrepancies between the observed frequencies and frequencies of unstable modes in models of DSCT stars. For example, the models of Xiong et al. (2016) predict frequencies that are far higher than observed.

It is found that there is a well-defined envelope for the frequency of maximum amplitude as a function of temperature. The same relationship is found if, instead of the frequency of maximum amplitude,  $\nu_1$ , the frequency of the  $n$ -th largest amplitude,  $\nu_n$ , is used. The maximum frequency and the frequency range is smallest in cool DSCT stars, but increases smoothly with temperature. The frequency reaches a maximum of about  $72 \text{ d}^{-1}$  at  $T_{\text{eff}} \approx 8500 \text{ K}$  then decreases.

The decrease in frequency and frequency range with temperature continues in the MAIA variables, eventually reaching a minimum at about  $T_{\text{eff}} \approx 18\,000 \text{ K}$ . The highest frequencies of unstable modes in DSCT models do have an upper limit in reasonable agreement with observations. This limit is related to the thermal timescale in the driving region. However, models do not predict unstable high frequencies in stars hotter than about  $8500 \text{ K}$ . The decrease in maximum frequency for stars hotter than this limit may provide a clue to the driving mechanism in MAIA variables.

The presence of equal numbers of DSCT and GDOR in the same region of the H–R diagram shows the pulsation mechanism must be the same in the two classes. The arbitrary frequency used to separate DSCT and GDOR stars has no physical significance. This seems to be just another example of the problem just described: very different frequency patterns can be produced by stars with similar parameters. Low frequencies are present in DSCT stars across the whole instability strip. The reason why the GDOR class was created can be attributed to the difficulty of detecting low frequencies with small amplitudes from the ground. Perhaps the GDOR class should be absorbed into the DSCT class.

It has been suggested that SPB variables cooler than the cool edge of the SPB instability strip can be explained by rapid rotation (Szewczuk and Daszyńska-Daszkiewicz 2012; Salmon et al. 2014). However, from 27 SPB stars cooler than  $11\,000 \text{ K}$ ,  $\langle v \sin i \rangle = 184 \pm 20 \text{ km s}^{-1}$ . From 397 main sequence stars in the same effective temperature range,  $\langle v \sin i \rangle = 124 \pm 5 \text{ km s}^{-1}$ . The anomalous SPB stars do not seem to be rotating rapidly.

The failure of pulsation models to describe the observations requires a re-assessment of the basic assumptions underlying the models. Perhaps there is more than one



driving mechanism active in upper main sequence stars. This might explain why DSCT and MAIA variables are seen over a very wide range of effective temperatures. It is also evident that a re-assessment of the current variability classes is required. However, this must await future investigations on pulsational driving among hot main sequence stars.

## ACKNOWLEDGMENTS

I wish to thank the National Research Foundation of South Africa for financial support.

## DATA AVAILABILITY

The data underlying this article can be obtained from <https://sites.google.com/view/tessvariables/home>, and also available through the author.

## REFERENCES

- E. Alecian, O. Kochukhov, V. Petit, J. Grunhut, J. Landstreet, M. E. Oksala, G. A. Wade, G. Hussain, et al. Discovery of new magnetic early-B stars within the MiMeS HARPSpol survey. *A&A*, 567:A28, July 2014. doi:10.1051/0004-6361/201323286.
- F. Anders, A. Khalatyan, A. B. A. Queiroz, C. Chiappini, J. Ardèvol, L. Casamiquela, F. Figueras, Ó. Jiménez-Arranz, C. Jordi, M. Monguió, M. Romero-Gómez, D. Altamirano, T. Antoja, R. Assaad, T. Cantat-Gaudin, A. Castro-Ginard, H. Enke, L. Girardi, G. Guiglion, S. Khan, X. Luri, A. Miglio, I. Minchev, P. Ramos, B. X. Santiago, and M. Steinmetz. Photo-astrometric distances, extinctions, and astrophysical parameters for Gaia EDR3 stars brighter than  $G = 18.5$ . *A&A*, 658:A91, February 2022. doi:10.1051/0004-6361/202142369.
- M. Asplund, N. Grevesse, A. J. Sauval, and P. Scott. The Chemical Composition of the Sun. *ARA&A*, 47:481–522, September 2009. doi:10.1146/annurev.astro.46.060407.145222.
- L. A. Balona. Rapidly oscillating TESS A-F main-sequence stars: are the roAp stars a distinct class? *MNRAS*, 510(4): 5743–5759, March 2022a. doi:10.1093/mnras/stac011.
- L. A. Balona. Identification and classification of TESS variable stars. *arXiv e-prints*, art. arXiv:2212.10776, December 2022b.
- L. A. Balona. Maia variables and other anomalies among pulsating stars. *Frontiers in Astronomy and Space Sciences*, 10:1266750, September 2023. doi:10.3389/fspas.2023.1266750.
- L. A. Balona and D. Ozuyar. Pulsation among TESS A and B stars and the Maia variables. *MNRAS*, 493(4):5871–5879, March 2020a. doi:10.1093/mnras/staa670.
- L. A. Balona and D. Ozuyar. TESS observations of Be stars: a new interpretation. *MNRAS*, 493(2):2528–2544, April 2020b. doi:10.1093/mnras/staa389.
- L. A. Balona, K. Krisciunas, and A. W. J. Cousins. Gamma-Doradus - Evidence for a New Class of Pulsating Star. *MNRAS*, 270:905–+, October 1994.
- L. A. Balona, A. Pigulski, P. D. Cat, G. Handler, J. Gutiérrez-Soto, C. A. Engelbrecht, F. Frescura, M. Briquet, J. Cuypers, J. Daszyńska-Daszkiewicz, P. Degroote, R. J. Dukes, R. A. García, E. M. Green, U. Heber, S. D. Kawaler, H. Lehmann, B. Leroy, J. Molenda-Żaowicz, C. Neiner, A. Noels, J. Nuspl, R. Østensen, D. Pricopi, I. Roxburgh, S. Salmon, M. A. Smith, J. C. Suárez, M. Suran, R. Szabó, K. Uytterhoeven, J. Christensen-Dalsgaard, H. Kjeldsen, D. A. Caldwell, F. R. Girouard, and D. T. Sanderfer. Kepler observations of the variability in B-type stars. *MNRAS*, 413: 2403–2420, June 2011. doi:10.1111/j.1365-2966.2011.18311.x.
- L. A. Balona, C. A. Engelbrecht, Y. C. Joshi, S. Joshi, K. Sharma, E. Semenko, G. Pandey, N. K. Chakradhari, et al. The hot  $\gamma$  Doradus and Maia stars. *MNRAS*, 460:1318–1327, August 2016. doi:10.1093/mnras/stw1038.
- Luis A. Balona. The extraordinary frequency pattern variation in  $\delta$  scuti stars. *The Open Journal of Astrophysics*, 7, 1 2024. doi:10.21105/astro.2109.12574.
- Luis A. Balona and Dogus Ozuyar. TESS Observations of Be Stars: General Characteristics and the Impulsive Magnetic Rotator Model. *ApJ*, 921(1):5, November 2021. doi:10.3847/1538-4357/ac1a77.
- S. Barceló Forteza, T. Roca Cortés, and R. A. García. The envelope of the power spectra of over a thousand  $\delta$  Scuti stars. The  $T_{\text{eff}} - \nu_{\text{max}}$  scaling relation. *A&A*, 614:A46, June 2018. doi:10.1051/0004-6361/201731803.
- S. Barceló Forteza, A. Moya, D. Barrado, E. Solano, S. Martín-Ruiz, J. C. Suárez, and A. García Hernández. Unveiling the power spectra of  $\delta$  Scuti stars with TESS. The temperature, gravity, and frequency scaling relation. *A&A*, 638:A59, June 2020. doi:10.1051/0004-6361/201937262.
- D. M. Bowman and D. W. Kurtz. Characterizing the observational properties of  $\delta$  Sct stars in the era of space photometry from the Kepler mission. *MNRAS*, 476:3169–3184, May 2018. doi:10.1093/mnras/sty449.
- S. Burssens, S. Simón-Díaz, D. M. Bowman, G. Holgado, M. Michielsen, A. de Burgos, N. Castro, R. H. Barbá, and C. Aerts. Variability of OB stars from TESS southern Sectors 1-13 and high-resolution IACOB and OWN spectroscopy. *A&A*, 639:A81, July 2020. doi:10.1051/0004-6361/202037700.
- E. Chapellier, D. Le Contel, J. M. Le Contel, P. Mathias, and J.-C. Valtier. A hybrid  $\beta$  Cephei-SPB star in a binary system:  $\gamma$  Pegasi. *A&A*, 448:697–701, March 2006. doi:10.1051/0004-6361:20053815.
- P. Degroote, C. Aerts, M. Ollivier, A. Miglio, J. Debosscher, J. Cuypers, M. Briquet, J. Montalbán, et al. CoRoT’s view of newly discovered B-star pulsators: results for 358 candidate B pulsators from the initial run’s exoplanet field data. *A&A*, 506: 471–489, October 2009. doi:10.1051/0004-6361/200911884.
- P. Degroote, C. Aerts, A. Baglin, A. Miglio, M. Briquet, A. Noels, E. Niemczura, J. Montalbán, S. Bloemen, R. Oreiro, M. Vučković, K. Smolders, M. Auvergne, F. Baudin, C. Catala, and E. Michel. Deviations from a uniform period spacing of gravity modes in a massive star. *Nature*, 464:259–261, March 2010. doi:10.1038/nature08864.
- M.-A. Dupret, A. Grigahcène, R. Garrido, M. Gabriel, and R. Scuflaire. Convection-pulsation coupling. II. Excitation and stabilization mechanisms in  $\delta$  Sct and  $\gamma$  Dor stars. *A&A*, 435: 927–939, June 2005. doi:10.1051/0004-6361:20041817.
- W. Dziembowski. Oscillations of giants and supergiants. *Acta Astronomica*, 27:95–126, 1977.
- W. A. Dziembowski and A. A. Pamyatnykh. The two hybrid B-type pulsators:  $\nu$  Eridani and 12 Lacertae. *MNRAS*, 385: 2061–2068, April 2008. doi:10.1111/j.1365-2966.2008.12964.x. URL <http://adsabs.harvard.edu/abs/2008MNRAS.385.2061D>.
- Gaia Collaboration, J. De Ridder, V. Ripepi, C. Aerts, L. Palaversa, L. Eyser, B. Holl, M. Audard, et al. Gaia Data Release 3. Pulsations in main sequence OBAF-type stars. *A&A*, 674:A36, June 2023. doi:10.1051/0004-6361/202243767.
- A. Grigahcène, V. Antoci, L. Balona, G. Catanzaro, J. Daszyńska-Daszkiewicz, J. A. Guzik, G. Handler, G. Houdek, et al. Hybrid  $\gamma$  Doradus- $\delta$  Scuti Pulsators: New Insights into the Physics of the Oscillations from Kepler Observations. *ApJ*, 713:L192–L197, April 2010. doi:10.1088/2041-8205/713/2/L192.
- J. A. Guzik, A. B. Kaye, P. A. Bradley, A. N. Cox, and C. Neuforge. Driving the Gravity-Mode Pulsations in  $\gamma$  Doradus Variables. *ApJ*, 542:L57–L60, October 2000. doi:10.1086/312908. URL <http://adsabs.harvard.edu/abs/2000ApJ...542L..57G>.
- G. Handler, L. A. Balona, R. R. Shobbrook, C. Koen, A. Bruch, E. Romero-Colmenero, A. A. Pamyatnykh, B. Willems, et al. Discovery and analysis of p-mode and g-mode oscillations in the A-type primary of the eccentric binary HD 209295. *MNRAS*, 333:262–279, June 2002. doi:10.1046/j.1365-8711.2002.05295.x.

- G. Handler, M. Jerzykiewicz, E. Rodríguez, K. Uytterhoeven, P. J. Amado, T. N. Dorokhova, N. I. Dorokhov, E. Poretti, J.-P. Sareyan, L. Parrao, D. Lorenz, D. Zsuffa, R. Drummond, J. Daszyńska-Daszkiewicz, T. Verhoelst, J. De Ridder, B. Acke, P.-O. Bourge, A. I. Movchan, R. Garrido, M. Paparó, T. Sahin, V. Antoci, S. N. Udovichenko, K. Csorba, R. Crowe, B. Berkey, S. Stewart, D. Terry, D. E. Mkrtychian, and C. Aerts. Asteroseismology of the  $\beta$  Cephei star 12 (DD) Lacertae: photometric observations, pulsational frequency analysis and mode identification. *MNRAS*, 365:327–338, January 2006. doi:10.1111/j.1365-2966.2005.09728.x. URL <http://adsabs.harvard.edu/abs/2006MNRAS.365..327H>.
- G. W. Henry, F. C. Fekel, and S. M. Henry. Photometry and Spectroscopy of 11  $\gamma$  Doradus Stars. *AJ*, 133:1421–1440, April 2007. doi:10.1086/511820. URL <http://adsabs.harvard.edu/abs/2007AJ...133.1421H>.
- M. Jerzykiewicz, G. Handler, R. R. Shobbrook, A. Pigulski, R. Medupe, T. Mokgwetsi, P. Tlhagwane, and E. Rodríguez. Asteroseismology of the  $\beta$  Cephei star  $\nu$  Eridani - IV. The 2003-2004 multisite photometric campaign and the combined 2002-2004 data. *MNRAS*, 360:619–630, June 2005. doi:10.1111/j.1365-2966.2005.09088.x. URL <http://adsabs.harvard.edu/abs/2005MNRAS.360..619J>.
- T. Kallinger, I. Iliev, H. Lehmann, and W. W. Weiss. The puzzling Maia candidate star  $\alpha$  Draconis. In J. Zverko, J. Ziznovsky, S. J. Adelman, & W. W. Weiss, editor, *The A-Star Puzzle*, volume 224 of *IAU Symposium*, pages 848–852, December 2004.
- D. W. Kurtz. Rapidly oscillating AP stars. *MNRAS*, 200:807–859, September 1982. URL <http://adsabs.harvard.edu/abs/1982MNRAS.200..807K>.
- J. Labadie-Bartz, G. Handler, J. Pepper, L. A. Balona, P. De Cat, D. J. Stevens, M. B. Lund, et al. New Beta Cephei Stars from the KELT Project. *AJ*, 160(1):32, July 2020. doi:10.3847/1538-3881/ab952c.
- H. Lehmann, G. Scholz, G. Hildebrandt, S. Klose, K. P. Panov, H.-G. Reimann, M. Woche, and R. Ziener. Variability investigations of possible Maia stars. *A&A*, 300:783, August 1995.
- B. J. McNamara. Maia variables and upper-main-sequence phenomena. *ApJ*, 289:213–219, February 1985. doi:10.1086/162881.
- A. Miglio, J. Montalbán, and M.-A. Dupret. Revised instability domains of SPB and  $\beta$  Cephei stars. *Communications in Asteroseismology*, 151:48–56, August 2007a. doi:10.1553/cia151s48. URL <http://adsabs.harvard.edu/abs/2007CoAst.151...48M>.
- Andrea Miglio, Josefina Montalbán, and Marc-Antoine Dupret. Instability strips of slowly pulsating B stars and  $\beta$  Cephei stars: the effect of the updated OP opacities and of the metal mixture. *MNRAS*, 375(1):L21–L25, Feb 2007b. doi:10.1111/j.1745-3933.2006.00267.x.
- Giovanni M. Mirouh. Forward modelling and the quest for mode identification in rapidly rotating stars. *Frontiers in Astronomy and Space Sciences*, 9:952296, October 2022. doi:10.3389/fspas.2022.952296.
- J. S. G. Mombarg, T. Van Reeth, M. G. Pedersen, G. Molenberghs, D. M. Bowman, C. Johnston, A. Tkachenko, and C. Aerts. Asteroseismic masses, ages, and core properties of  $\gamma$  Doradus stars using gravito-inertial dipole modes and spectroscopy. *MNRAS*, 485(3):3248–3263, May 2019. doi:10.1093/mnras/stz501.
- E. Moravveji. The impact of enhanced iron opacity on massive star pulsations: updated instability strips. *MNRAS*, 455:L67–L71, January 2016. doi:10.1093/mnras/ltv142.
- Mohammed Mourabit and Nevin N. Weinberg. Resonant Mode Coupling in  $\delta$  Scuti Stars. *ApJ*, 950(1):6, June 2023. doi:10.3847/1538-4357/acca16.
- R. M. Ouazzani, F. Lignières, M. A. Dupret, S. J. A. J. Salmon, J. Ballot, S. Christophe, and M. Takata. First evidence of inertial modes in  $\gamma$  Doradus stars: The core rotation revealed. *A&A*, 640:A49, August 2020. doi:10.1051/0004-6361/201936653.
- B. Paczyński. Evolution of Single Stars. I. Stellar Evolution from Main Sequence to White Dwarf or Carbon Ignition. *Acta Astronomica*, 20:47, 1970.
- A. A. Pamyatnykh, G. Handler, and W. A. Dziembowski. Asteroseismology of the  $\beta$  Cephei star  $\nu$  Eridani: interpretation and applications of the oscillation spectrum. *MNRAS*, 350:1022–1028, May 2004. doi:10.1111/j.1365-2966.2004.07721.x. URL <http://adsabs.harvard.edu/abs/2004MNRAS.350.1022P>.
- P. I. Pápics, M. Briquet, A. Baglin, E. Poretti, C. Aerts, P. Degroote, A. Tkachenko, T. Morel, et al. Gravito-inertial and pressure modes detected in the B3 IV CoRoT target HD 43317. *A&A*, 542:A55, June 2012. doi:10.1051/0004-6361/201218809.
- J. R. Percy and J. B. Wilson. Another Search for Maia Variable Stars. *PASP*, 112:846–851, June 2000. doi:10.1086/316577. URL <http://adsabs.harvard.edu/abs/2000PASP..112..846P>.
- A. Pigulski and G. Pojmański.  $\beta$  Cephei stars in the ASAS-3 data. II. 103 new  $\beta$  Cephei stars and a discussion of low-frequency modes. *A&A*, 477:917–929, January 2008. doi:10.1051/0004-6361:20078581.
- F. J. Rogers and C. A. Iglesias. Radiative atomic Rosseland mean opacity tables. *ApJS*, 79:507–568, April 1992. doi:10.1086/191659.
- H. Saio, D. W. Kurtz, S. J. Murphy, V. L. Antoci, and U. Lee. Theory and evidence of global Rossby waves in upper main-sequence stars: r-mode oscillations in many Kepler stars. *MNRAS*, 474:2774–2786, February 2018. doi:10.1093/mnras/stx2962.
- S. J. A. J. Salmon, J. Montalbán, D. R. Reese, M.-A. Dupret, and P. Eggenberger. The puzzling new class of variable stars in NGC 3766: old friend pulsators? *A&A*, 569:A18, September 2014. doi:10.1051/0004-6361/201323259.
- Xiang-dong Shi, Sheng-bang Qian, Li-ying Zhu, Liang Liu, Lin-jia Li, and Lei Zang. Observational Properties of 155 O- and B-type Massive Pulsating Stars. *ApJS*, 265(2):33, April 2023. doi:10.3847/1538-4365/acba91.
- A. Stankov and G. Handler. Catalog of Galactic  $\beta$  Cephei Stars. *ApJS*, 158:193–216, June 2005. doi:10.1086/429408. URL <http://adsabs.harvard.edu/abs/2005ApJS...158..193S>.
- W. Szewczuk and J. Daszyńska-Daszkiewicz. Identification of pulsational modes in rotating slowly pulsating B stars. *Astronomische Nachrichten*, 333:942, December 2012. doi:10.1002/asna.201211822.
- R. H. D. Townsend. Kappa-mechanism excitation of retrograde mixed modes in rotating B-type stars. *MNRAS*, 364(2):573–582, December 2005. doi:10.1111/j.1365-2966.2005.09585.x.
- T. Van Reeth, J. S. G. Mombarg, S. Mathis, A. Tkachenko, J. Fuller, D. M. Bowman, B. Buysschaert, C. Johnston, et al. Sensitivity of gravito-inertial modes to differential rotation in intermediate-mass main-sequence stars. *A&A*, 618:A24, October 2018. doi:10.1051/0004-6361/201832718.
- D. R. Xiong, L. Deng, C. Zhang, and K. Wang. Turbulent convection and pulsation stability of stars - II. Theoretical instability strip for  $\delta$  Scuti and  $\gamma$  Doradus stars. *MNRAS*, 457:3163–3177, April 2016. doi:10.1093/mnras/stw047.
- M. Zboril and P. North. He, CNO abundances and  $v \sin i$  values in He-rich stars. *Contributions of the Astronomical Observatory Skalnaté Pleso*, 30(1):12–20, April 2000.

provides fast and easy peer review for new papers in the astro-ph section of the arXiv, making the reviewing process simpler for authors and referees alike. Learn more at <http://astro.theoj.org>.

This paper was built using the Open Journal of Astrophysics L<sup>A</sup>T<sub>E</sub>X template. The OJA is a journal which